ISSN 0036-0244, Russian Journal of Physical Chemistry A, 2017, Vol. 91, No. 10, pp. 2039–2043. © Pleiades Publishing, Ltd., 2017.

PHOTOCHEMISTRY AND MAGNETOCHEMISTRY

Investigation of the Structural Properties of Annealed $CdIn_2Te_4$/CdS Thin Film Solar Cells Produced by the Electron-Beam Evaporation (e-Beam) Technique[1]

İbrahim Kırbaş* and Rasim Karabacak

Pamukkale University, Engineering Faculty, Mechanical Engineering Department, Kınıklı Campus, 20070 Denizli, Turkey

**e-mail: ikirbas428@gmail.com*

Received May 20, 2016

Abstract—Thin film $CdIn_2Te_4$/CdS solar cells were deposited onto the ITO-coated glass substrate by electron beam evaporation (e-beam) technique, and the the effect of annealing on their structural properties is studied. The annealing was performed under nitrogen atmosphere for 1 h. The manufactured solar cells were studied by X-ray diffraction (XRD), scanning electron microscopy (SEM) and energy dispersive X-ray (EDAX) analysis. Crystallite size (D), inter-planer distance (d) and lattice constant (a) values were calculated for the thin film solar cell from XRD data. Annealed samples display well defined XRD patterns with three diffraction peaks. We observed increased peak intensity in the annealed films. EDAX analysis showed that only $CdIn_2Te_4$ is present in absorber layer and CdS is found in the window layer, but no impurity atoms are present the structure. It is observed that surface roughness of the annealed films incresed, according to SEM images. The *I–V* characteristics show that the current is increased for annealed thin films solar cells.

Keywords: thin films, electron beam evaporation, structural properties, semiconductors, X-ray diffraction (XRD)

DOI: 10.1134/S0036024417100168

1. INTRODUCTION

In recent years, thin films attract attention. Because of it is a potential application in semiconducting devices, photovoltaic optoelectronic devices, solar energy converters, and nanodevices [1–3]. Electron-beam evaporation plays important role in film properties such crystal structure, the storage density, surface roughness [4]. Several potential ternary semiconductors for photovoltaic applications are investigated. Band gap and lattice parameter may be varied by changing the composition of these materials is important. On the other hand some of these types of ternary compounds $II–III_2–VI_4$ example $CdIn_2Te_4$ has attracted attention in recent. $CdIn_2Te_4$ energy band gap 1.1 eV is compound semiconductor, the structure is mainly chalcopyrite structure [5].

Many depositing technique, wet chemical method [3], electrochemical deposition [5], thermal evaporation [6], close-space vapor transport [7, 8], chemical bath deposition [9], Bridgman method [10, 11], $CdIn_2Te_4$ films were used to prepared. Different properties of the $CdIn_2Te_4$ films were investigated various in articles [12–14] but more information is needed. Solar cells are manufactured by being deposited $CdIn_2Te_4$/CdS on ITO-coated glass substrate with e-beam technique for the first time in the literature. The effect of annealing on the structural characteristics of these solar cells was examined.

2. EXPERIMENTAL DETAILS

2.1. Materials and Methods

ITO-coated glass substrate by e-beam system after being placed on the retention of graphite crucibles of polycrystalline materials in powder form was placed in a water-cooled crucible cabin. With reference to 2×10^{-5} Torr was passed to the vacuum value is reached, the storage process. First it was commissioned substrate rotation. It was introduced starting from the current 2 mA. Evaporation rate during storage was kept in approximately 25–35 Å/s. The system automatically ended when the thickness of 1 μm, the storage process by turning off the circuit breaker. $CdIn_2Te_4$ deposited substrates were annealed for 1 h in a PROTHERM brand horizontal furnace, which was heated up to 400°C and maintained in a nitrogen atmosphere [15]. The glass/ITO/$CdIn_2Te_4$ structure was formed, annealed and as-deposited samples were placed in the

[1] The article is published in the original.

e-beam system. After the CdS was placed into the graphite crucible in the form of a powder of 99.999% purity, the system was closed. Reference to 2×10^{-5} Torr thickness 1 μm value until it reaches the deposition pressure was carried out. After the glass/ITO/$CdIn_2Te_4$/CdS structure was formed, annealed and as-deposited samples were In contacts.

2.2. Physical Characterization and Electrochemical Measurements

ITO-coated glass was used as the substrate material. $CdIn_2Te_4$/CdS were obtained 1.44 cm^2 active area in the solar cells. The surface morphology and composition of the films was obtained through scanning electron microscopy (SEM) and energy dispersive X-ray (EDAX) analysis with a QUANTA (FEG-250) model. X-ray diffraction measurements were taken using a BRUKER XRD system (D8 Advance). The current–voltage characteristic in dark was measured by Keithley 2400 source meter.

3. RESULTS AND DISCUSSION

3.1. Structural Analysis

A $CdIn_2Te_4$/CdS (E0) thin film solar cell and $CdIn_2Te_4$/CdS (E400) thin film solar cell which was annealed for 1 h at 400°C were deposited onto the ITO substrate by e-beam evaporation. Figure 1 shows the XRD diffractions of E0 and E400 thin film solar cells. E0 samples it was observed in the XRD 2θ = 31.1° and 48.7°, including two peaks. These peaks are corresponded, respectively to the diffraction lines produced by the (202) and (311) crystalline planes. E400 samples display well defined XRD patterns with three diffraction peaks. We observed increased peak intensity in the annealed films. Respectively was 2θ = 24.5°, 28.2°, and 39.1°. These peaks are corresponded, respectively to the diffraction lines produced by the (111), (200), and (220) crystalline planes. Increase in the peak intensity due to annealing, this may be due to the thin films passing from an amorphous structure to a polycrystalline structure, and it may be an indication of decreasing structural deficiency [9].

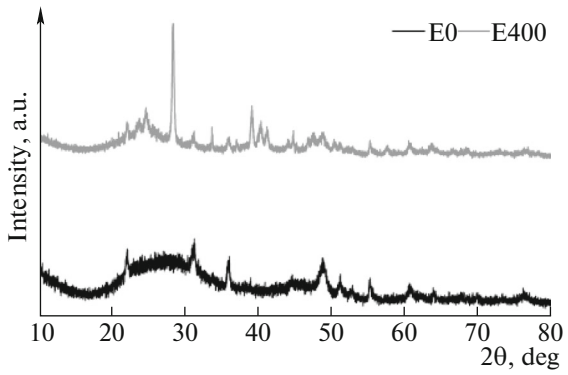

Fig. 1. The X-ray diffraction patterns of as-deposited (E0) and annealed (E400) thin film solar cells.

The crystallite sizes of thin films were calculated with XRD data using the Scherrer formula [16].

$$D = \frac{k\lambda}{\beta \cos\theta}, \quad (1)$$

where D is the crystal size, λ is the wavelength of the X-ray source, β is half the maximum width of the diffraction peak in radians, θ is the Bragg angle XRD diffraction peak, and k is a constant related to the film whose particle size was calculated [16].

The lattice constant (a) for cubic samples was calculated using the relation: $a = d(h^2 + k^2 + l^2)^{0.5}$, where h, k, l are the lattice planes and d is the inter-planar distance, measured using Bragg equation [3]. E0 and E400 values calculated for thin film solar cells are given in Table 1. Increased crystallite size was determined due to annealing, which means that films passed from an amorphous to a polycrystalline state. The detected crystallite size is consistent with those of other studies in the literature [6, 16]. The inter-planar distance (d) calculations are similar to those obtained by Jain et al. [5], and the lattice constant a

Table 1. Inter-planar distance (d), the lattice constant (a), and crystallite size (D) of E0 and E400 samples

Samples E0					Samples E400				
2θ, deg	*hkl*	*d* (Å)	*a* (Å)	*D* (nm)	2θ, deg	*hkl*	*d* (Å)	*a* (Å)	*D* (nm)
31.1	(202)[a]	2.870	8.117	21.0	24.5	(111)[c]	3.626	6.280	12.67
48.7	(311)[b]	1.866	6.188	8.43	28.2	(200)[d]	3.154	6.308	22.51
					39.1	(220)[e]	2.300	6.506	22.01

[a] [9].
[b] [3].
[c] [3, 5, 7, 17].
[d] [9].
[e] [3, 5, 17].

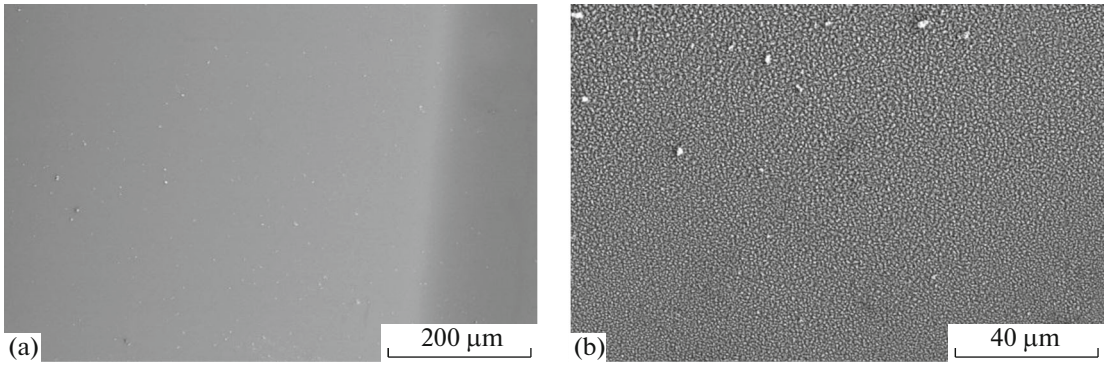

Fig. 2. (a) The SEM image of E0 and (b) the SEM image of E400.

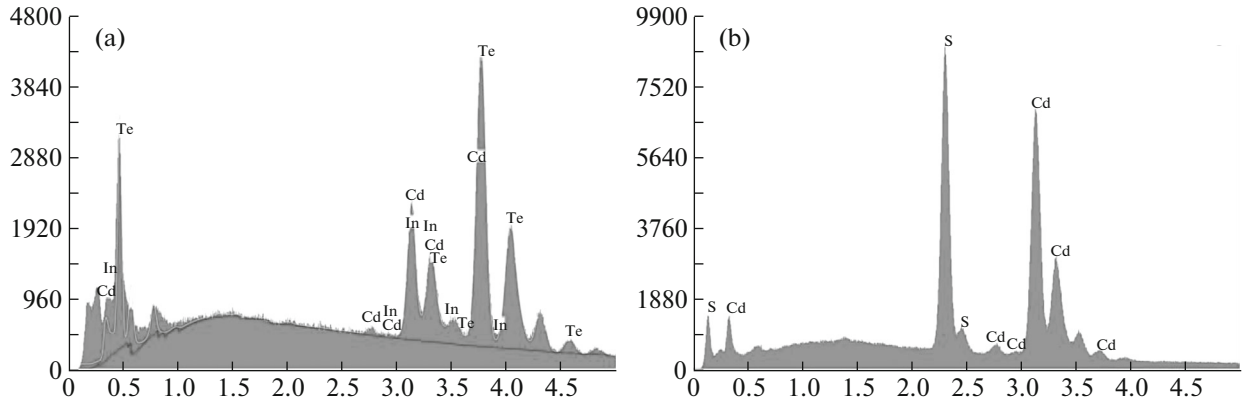

Fig. 3. Energy dispersive X-ray (EDAX) spectrums taken for the as-deposited thin film (a) $CdIn_2Te_4$ layer (b) CdS layer.

calculations are similar to those obtained by Mishra and Ganguli [12].

3.2. Surface Morphology Analysis

In order to determine the morphology of the surface material for annealed and as deposited solar cells SEM images are shown in Fig. 2. Figure 2 displays have increased surface roughness of the annealed film when examined. Similar behavior has been reported by Pandey et al. [18].

Table 2. EDS results of the absorber layer ($CdIn_2Te_4$)

	Elements	Average weight %	Atomic weight %
E0	Cd	17.17	18.94
	In	5.10	5.50
	Te	77.74	75.55
E400	Cd	17.74	19.55
	In	5.25	5.66
	Te	77.02	74.79

3.3. Composition Analysis

Energy dispersive X-ray (EDAX) spectrum of the annealed and as-deposited samples is shown in Figs. 3 and 4.

In this study $CdIn_2Te_4$ as absorber layer at 99.999% purity CdS (in powder form) was used as the window layer material. Materials were deposited on an ITO-coated glass substrate by e-beam evaporation technique. The deposited thin film solar cell EDS analysis results are shown in Tables 2 and 3. An increase in the Cd and In ratio and a decrease in Te ratio was observed in the deposited absorber layer obtained by the e-beam evaporation technique after annealing. The Cd and S

Table 3. EDS results of the window layer (CdS)

	Elements	Average weight %	Atomic weight %
E0	Cd	76.48	55.20
	S	23.52	44.80
E400	Cd	83.68	53.63
	S	16.32	46.37

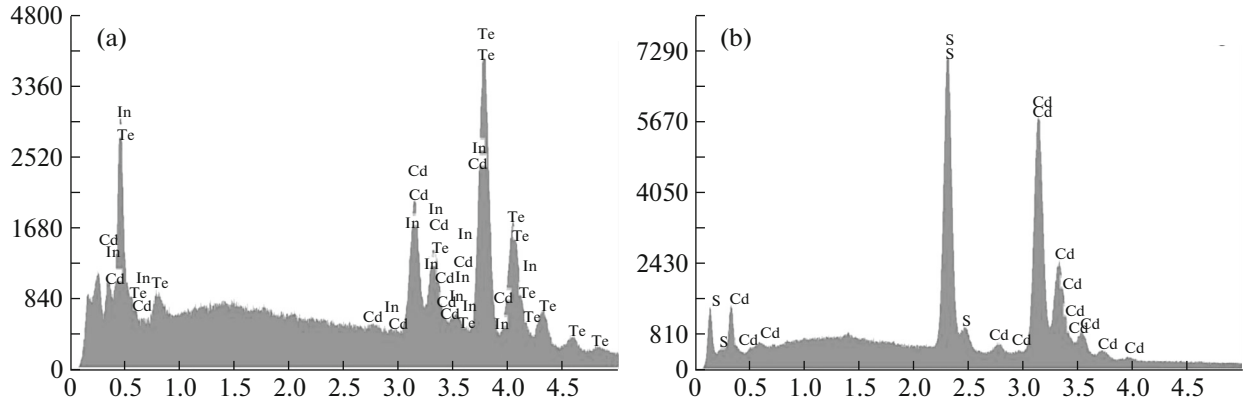

Fig. 4. Energy dispersive X-ray (EDAX) spectrums taken for the annealed thin film (a) $CdIn_2Te_4$ layer (b) CdS layer.

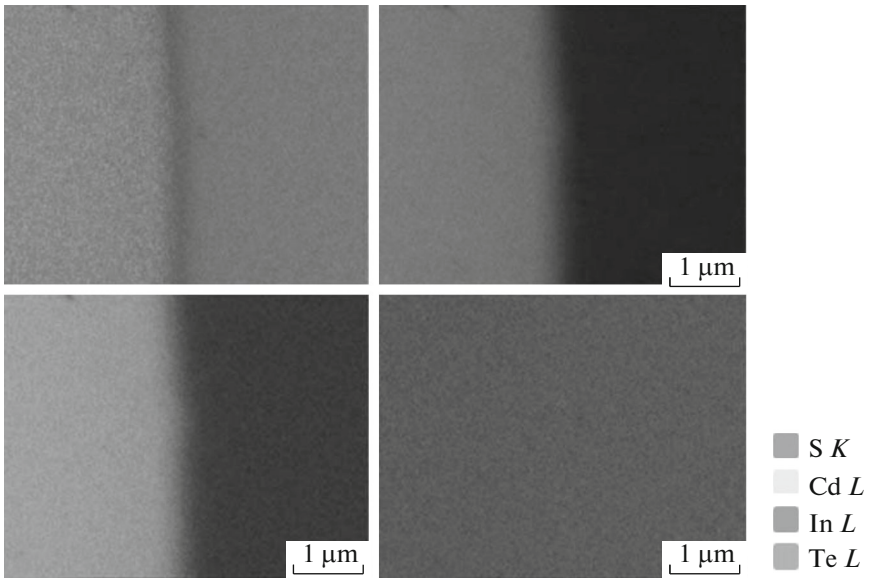

Fig. 5. Element placement.

values for the window layer material are consistent with the results of the study by Rmili et al. [19].

Figure 5 shows the absence of impurity atoms in the structure. The absorber layer consists of Cd, In, and Te atoms, and the window layer consists of Cd and S atoms.

3.4. Electrical Analysis

The transverse current–voltage characteristics of as-deposited and annealed $CdIn_2Te_4$ thin films solar cells are presented in Fig. 6. It is clearly visible in Fig. 6 that the variation in current with voltage for as-deposited and annealed $CdIn_2Te_4$ thin films solar cells is found to be linear. It is observed that the current of the solar cells is found to be increased for annealed solar cells. The results are well agreed with earlier reported work [20].

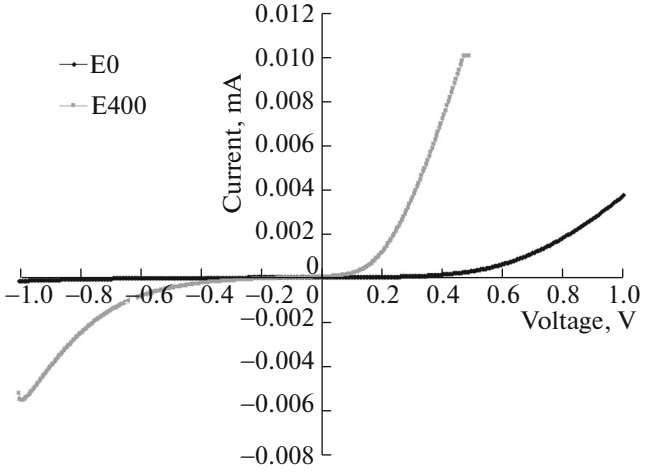

Fig. 6. Dark *I–V* characteristics of as-deposited and annealed $CdIn_2Te_4$/CdS thin films solar cells.

4. CONCLUSIONS

The e-beam technique was used to form *p*-$CdIn_2Te_4$ and *n*-CdS structures on an ITO-coated glass substrate. Thin-film solar cells were annealed at 400°C, and as-deposited thin-film solar cells were investigated to determine their structural properties. Through XRD analysis, as-deposited solar cells were found in the direction of (202) and (311). Annealed solar cells were found in the direction of (111), (200), and (220). This indicates the transition from an amorphous to a polycrystalline structure. The largest peak position $2\theta = 31.1°$ for as-deposited solar cells and annealed solar cells it has been identified as $2\theta = 28.2°$. Particle size was also calculated; annealed films were found to have increased particle size, whereas a polycrystalline structure to become clearer. In addition, the inter-planar distance *d* and lattice constant *a* values were calculated using Bragg's law. The determined values were found to be in agreement with literature. SEM and EDAX analysis showed an increase in surface roughness of the annealed solar cells and no impurity atom in structure. The *I–V* characteristics show that the current is increased for annealed thin films solar cells.

ACKNOWLEDGMENTS

This work was financially supported by the Scientific Research Projects Center (BAP) of Pamukkale University (project no. 2014FBE007).

REFERENCES

1. R. Chandramohan, T. Mahalingam, J. P. Chu, and P. J. Sebastian, Solar Energy Mater. Solar Cells **81**, 371 (2004).
2. S. K. Deshmukh, A. V. Kokate, and D. J. Sathe, Mater. Sci. Eng. B **122**, 206 (2005).
3. A. Y. Shenouda, M. M. Rashad, and L. Chow, J. Alloys Compd. **563**, 39 (2013).
4. S. Shanmugan and D. Mutharasu, Mater. Sci. Semicond. Process. **13**, 298 (2010).
5. K. Jain, R. K. Sharma, S. Kohli, K. N. Sood, and A. C. Rastogi, Curr. Appl. Phys. **3**, 251 (2003).
6. K. Yılmaz and D. Gölcür, SDU J. Sci. **9**, 150 (2014).
7. M. Zapata-Torres, R. Castro-Rodriguez, M. Melendez-Lira, and S. Jimenez-Sandoval, A. Zapata-Navarro, and J. L. Pena, Thin Solid Films **358**, 12 (2000).
8. A. Iribarren, I. Riech, M. P. Hernandez, R. Castro-Rodriguez, J. L. Pena, and M. Zapata-Torres, J. Vacuum Sci. Technol. A **17**, 3433 (1999).
9. M. Singsangah, K. Hongsith, S. Choopun, and A. Tubtimtae, J. Colloid Interface Sci. **451**, 189 (2015).
10. S. H. You, K. J. Hong, T. S. Jeong, C. J. Youn, J. S. Park, D. C. Shin, and J. D. Moon, J. Cryst. Growth **256**, 116 (2003).
11. K. Hong, J. Korean Phys. Soc. **45**, 496 (2004).
12. S. Mishra and B. Ganguli, Mater. Chem. Phys. **173**, 429 (2016).
13. M. Quintero, E. Guerrero, R. Tovar, M. Morocoıma, and P. Grima, J. Phys. Chem. Solids **57**, 271 (1996).
14. M. Quintero, J. Phys. Chem. Solids **58**, 497 (1997).
15. B. V. Rajendra and D. Kekuda, J. Mater. Sci.: Mater. Electron. **23**, 1805 (2012).
16. M. M. El-Nahass, G. M. Youssef, and S. Z. Noby, J. Alloys Compd. **604**, 253 (2014).
17. R. Ramirez-Bon, R. Nunez-Lopez, F. J. Espinoza-Beltran, O. Zelaya-Angel, and J. Gonzalez-Hernandez, J. Phys. Chem. Solids **58**, 807 (1997).
18. S. K. Pandey, U. Tiwari, R. Raman, C. Prakash, V. Krishna, V. Dutta, and K. Zimik, Thin Solid Films **473**, 54 (2005).
19. A. Rmili, F. Ouachtari, A. Bouaoud, A. Louardi, T. Chtouki, B. Elidrissi, and H. Erguig, J. Alloys Compd. **557**, 53 (2013).
20. S. Singh, R. Kumar, and K. N. Sood, Thin Solid Films **519**, 1078 (2010).